

Technical Notes

TECHNICAL NOTES are short manuscripts describing new developments or important results of a preliminary nature. These Notes should not exceed 2500 words (where a figure or table counts as 200 words). Following informal review by the Editors, they may be published within a few months of the date of receipt. Style requirements are the same as for regular contributions (see inside back cover).

Experimental Study of the Nozzle Surface Regression Rate to the Heat Transfer

Tae-Ho Lee*

Agency for Defense Development,
Daejeon 305-600, Republic of Korea

Introduction

THE thermal insulators (sacrificial materials) are used for the inside wall of the nozzle to maintain the original contour for the good performance of rocket motors. The properties of the thermal insulators vary depending on the raw material and manufacturing process.¹

The insulating material is eroded by the hot flowing gas during the combustion. There are mainly three causes of surface regression. But it is not simple to predict or measure the regression amount separately,^{2,3} and it is more useful for the practical point of view to get the total amount of regression; therefore, in this study the total regression rate was investigated.

In this analysis, carbon/phenolic MK4926 (manufactured by Hankook Fiber Glass Company, Korea) was investigated, which was 90 deg stack molded. For the temperature prediction of the structure, the well-known Bartz equation⁴ was adopted, but the radiation heat-transfer effect is not involved, simply because the radiation heat transfer is one order of magnitude smaller than the convective heat transfer even at the starting part of the convergent nozzle section.⁵ For the mechanical erosion, the Reynolds analogy was adopted in order to get the relationship between the heat transfer and the shear stress.

Analysis

At the nozzle wall the heat flux contributing to surface regression, if the mechanism of material removal is ablation, is given by

$$\eta h_c (T_{aw} - T_a) = \lambda_a \rho \dot{r}_a \quad (1)$$

where \dot{r} represents regression rate and subscript a means the ablation.

At a given conditions, the ablation rate equation can be simplified as follows:

$$\dot{r}_a = C_1 h_c \quad (2)$$

Actually, the decomposition products that enter the gas stream thicken the boundary layer and lower the value of the heat-transfer coefficient; however, this blowing effect is negligible.⁶

Presented as Paper 2004-3388 at the AIAA/ASME/SAE/ASEE 40th Joint Propulsion Conference, Broward County Convention Center Fort Lauderdale, FL, 11–14 July 2004; received 21 July 2004; revision received 23 June 2005; accepted for publication 30 June 2005. Copyright © 2005 by the American Institute of Aeronautics and Astronautics, Inc. All rights reserved. Copies of this paper may be made for personal or internal use, on condition that the copier pay the \$10.00 per-copy fee to the Copyright Clearance Center, Inc., 222 Rosewood Drive, Danvers, MA 01923; include the code 0748-4658/06 \$10.00 in correspondence with the CCC.

*Head, Principal Researcher, Propulsion Department.

It is shown the linear relationship between the mechanical erosion rate \dot{r}_m and the usual group in fluid dynamics, that is to say, $\tau_w / \rho c^*$, where ρ is the average density of gases and c^* is their characteristic velocity.⁷

$$\dot{r}_m \propto \tau_w / \rho c^* \quad (3)$$

Simply it will be assumed that the erosion temperature is constant. Then the mechanical erosion rate can be expressed as follows by similarity as the ablation:

$$\dot{r}_m = \beta \tau_w \quad (4)$$

If one accepts Reynolds analogy between heat and mass transfer and assumes that driving potential (concentration gradient for the reactive species) for corrosion is weakly dependent on the wall temperature, then the corrosion rate will again be proportional to the heat-transfer coefficient.

Therefore the total surface regression rate is expressed as follows:

$$\dot{r} = \alpha h_c + \beta \tau_w \quad (5)$$

where α includes the C_1 in Eq. (2) and the constant of the chemical corrosion together

Heat Transfer and Shear Stress

Bartz derived a semi-experimental closed-form heat-transfer coefficient equation using integral momentum and energy equations:

$$h_c = \left[\frac{0.026}{D_t^{0.2}} \left(\frac{\mu_o^{0.2} C_p}{Pr^{0.6}} \right) \left(\frac{P_o g}{c^*} \right)^{0.8} \left(\frac{D_t}{r_c} \right)^{0.1} \right] \left(\frac{A_t}{A} \right)^{0.9} \sigma \quad (6)$$

It is assumed that both C_p and Pr are constant over the boundary layer, the properties whose variations must be accounted for, are only ρ and μ , and these variable properties can be compensated across the boundary layer using properties correction factor σ . This correction factor σ is expressed differently depending on choosing the reference temperature⁸ at which the boundary-layer gas properties are evaluated. The midtemperature of the freestream gas and the wall or the Eckert reference temperature will be used for the reference temperature.

At the given nozzle contour, the cross-section area ratio (A_t/A) is fixed; therefore, Eq. (6) can be expressed without temperature dependency if the properties correction factor σ does not involve the temperature ratio. Then Eq. (6) is shortened as follows:

$$h_c = h_0 (A_t/A)^n \quad (7)$$

where h_0 is the big bracket term in Eq. (6). Now let $(A_t/A)^n$ be a geometric factor, then Eq. (7) involves only geometric factor $(A_t/A)^n$, which comes from the multiplication of the properties correction factor σ and $(A_t/A)^{0.9}$; the multiplication value $\sigma (A_t/A)^{0.9}$ is called in here the geometric correction factor. The geometric factor index n is used 0.8 through curve fit in this analysis at the convergent part. The comparison of the geometric factor $(A_t/A)^{0.8}$ in Eq. (7) and geometric correction factor $\sigma (A_t/A)^{0.9}$ using the different reference temperature for $\gamma = 1.2$ is shown in Fig. 1.

Now, von Kármán type Reynolds analogy is adopted between the Stanton number and the skin-friction coefficient in order to express

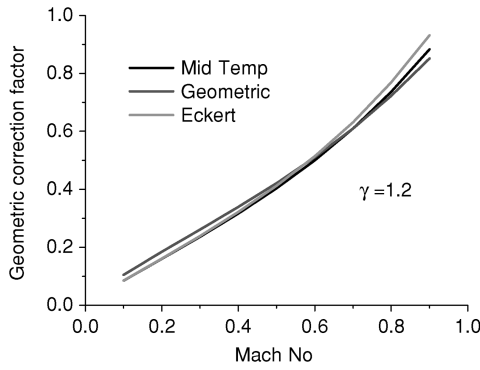


Fig. 1 Mach number vs geometric factor for $\gamma = 1.2$.

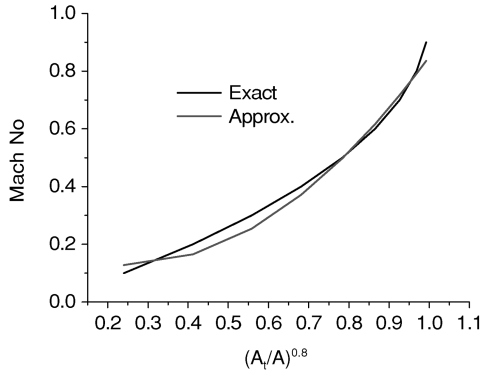


Fig. 2 Approximation of the Mach number and geometric factor.

the gas dynamic shear stress by the heat-transfer coefficient, then the shear stress is expressed as follows:

$$\tau_w = C_2 u_\infty h_c \quad \text{or} \quad \tau_w = C M h_c \quad (8)$$

where C_2 and C are constants. For the given chamber condition and nozzle shape, the freestream gas velocity can be converted to Mach number. The Mach number and h_c are also functions of nozzle geometry; therefore, the Mach number can be expressed by h_c using geometric relations. To do so, the following relation is used:

$$M = g[h_c, \gamma] = f[(A_t/A)^{0.8}, \gamma] \quad (9)$$

For the convergent section, second-order polynomial form of (A_t/A) is used to express the Mach number by the least-square fit at the given nozzle section area. The Mach number and $(A_t/A)^{0.8}$ relation is shown in the Fig. 2.

$$M = 1.25X^2 - 0.6X + 0.2 \quad (10)$$

where X is $(A_t/A)^{0.8}$. The local convective heat-transfer coefficient varies with $(A_t/A)^{0.8}$, and Mach number also depends on $(A_t/A)^{0.8}$. Using Eqs. (8) and (10), the total surface regression rate Eq. (5) is expressed as follows:

$$\dot{r} = a_1 h_c + a_2 (1.25 h_c^2 - 0.6 h_c + 0.2) h_c + a_0 \quad (11)$$

By the experimental data, the preceding equation coefficients a will be determined.

Experiment and Results

To get the regression amount, three small size end-burning motors were ground tested. These motors were loaded with the hydroxyl-terminated polybutadiene composite propellant, which had no aluminium component, and as the insulation material the carbon-fiber-reinforced plastics with phenolic resin was chosen. This insulator was 90-deg stack molded by Hankook Fiber Glass Company in Korea. The dimensions and characteristics of these tested motors and nozzles are shown in Table 1. During the burning time, the chamber

Table 1 Dimensions and characteristics of test motors and nozzles

Motor no.	Motor 1	Motor 2	Motor 3
Pc, kPa	3.95	0.86	3.17
Burn time, s	39	110	58.2
Length of grain, mm	777	777	970
Throat dia., mm	15.7	20.2	15.8
Nozzle-exit dia., mm	33	33	33

Table 2 Nozzle surface regression rate and heat-transfer coefficient

Motor 1		Motor 2		Motor 3	
h_c , w/m ² k	\dot{r} , mm/s	h_c , w/m ² k	\dot{r} , mm/s	h_c , w/m ² k	\dot{r} , mm/s
1286.26	0.023	538.38	0.005	1087.95	0.026
1730.46	0.031	724.30	0.041	1463.66	0.029
2236.55	0.044	936.13	0.023	1891.72	0.034
2586.98	0.051	1082.80	0.020	2188.11	0.029
3036.25	0.051	1270.85	0.027	2568.12	0.052
3805.13	0.077	1592.67	0.029	3218.45	0.060
4949.24	0.141	2071.54	0.029	4186.16	0.086
5933.18	0.115	2483.38	0.036	5018.40	0.095
7279.73	0.115	3046.99	0.037	6157.33	0.098

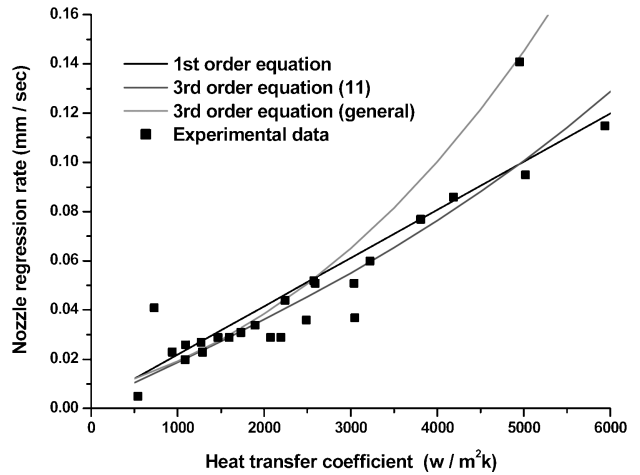


Fig. 3 Heat-transfer coefficient and regression rate.

pressure, thrust, and the structure skin temperature were measured, and the amount of the surface regression was measured after cutting the nozzle. The regression amount is almost constant along the circumferential direction at the given local point of the convergent section, but at the divergent section it is not axisymmetrical, and there are some deviations. In this analysis, the consideration is limited only for the convergent part.

Table 2 shows the heat-transfer coefficient that was predicted by Eq. (6) and the surface regression amount of these motor nozzles.

The heat-transfer coefficients and the surface regression amount of these tested motors are altogether plotted, even though the chamber pressure and burning time are different. Then these experimental data are curve fitted by using the least-square method. Even though different polynomials are used, the error norms are same order for all three. The first order of h_c (convective heat transfer) and third-order equations and general third-order form are also shown in Fig. 3.

The experimental results show that the ablation, including some kind order of a chemical corrosion, is the dominant mechanism that is represented by first order of convective heat-transfer coefficient. Comparing this, the mechanical erosion that is expressed by higher-order polynomials of h_c is much small. In other words, the experimental results give that the mechanical erosion mechanism is negligible for this carbon fiber reinforced plastics stack molded insulator, and the dominant mechanism of the regression is ablation at the convergent section of nozzle. It is thought that at the convergent part the gas velocity is subsonic; therefore, the gas dynamic shear stress affects little.

Figure 3 shows that the surface regression rate can be expressed by first-order polynomials without losing accuracy the same as the third-order polynomials. The coefficient of the higher-order term is less by 10 than the first-order value. But at the divergent part, the high-order coefficient, which might be represented the mechanical erosion, will not be negligible as the convergent part because the regression trend increases even as the heat-transfer coefficient decreases.

Conclusions

The conclusions can be summarized as follows:

The geometric factor $(A_t/A)^{0.8}$ represents the multiplication value of the properties correction factor and area ratio well. And shear stress, which will affect the erosion rate, has a relation to the heat-transfer coefficient by freestream Mach number through von Kármán analogy. The ablation mechanism including the chemical corrosion, which is represented by first-order h_c , is the dominant one comparing the mechanical erosion that is represented by higher-order polynomials of h_c .

The surface regression rate might be expressed only by the first-order function of heat-transfer coefficient without losing the accuracy at the convergent part of the nozzle.

References

- ¹Fairall, R. S., Clark, L. C., Davis, H. O., and Shefil, L., "The Mechanism of Insulation Surface Regression in Rocket Motors," *Aerospace Chemical Engineering*, Vol. 62, No. 61, 1964, pp. 44–54.
- ²Marthieu, R. D., "Mechanical Spallation of Charring Ablators in Hypersonic Environments," *AIAA Journal*, Vol. 2, No. 9, 1964, pp. 1621–1627.
- ³Schneider, P. J., Dolton, T. A., and Reed, G. W., "Mechanical Erosion of Charring Ablators in Grounds Test and Re-Entry Environments," *AIAA Journal*, Vol. 6, No. 1, 1968, pp. 64–72.
- ⁴Bartz, D. R., "Turbulent Boundary Layer Heat Transfer from Rapidly Accelerating Flow of Rocket Combustion Gases," *Advances in Heat Transfer*, edited by J. P. Hartnett and T. F. Irvine, Jr., Vol. 2, Academic Press, New York, 1965, pp. 11–109.
- ⁵Cornolisse, J. W., Schoyer, H. F. R., and Wakker, K. F., "Heat Transfer in the Rocket Motor," *Rocket Propulsion and Spaceflight Dynamics*, 1st ed., Pitman, London, 1979, pp. 160–166.
- ⁶Chung, J. N., and Lee, Tae-Ho, "A Mathematical Model of Condensation Heat and Mass Transfer to a Moving Droplet in its Own Vapor," *Journal of Heat Transfer*, Vol. 106, No. 2, 1984, pp. 417–424.
- ⁷Gowariker, V. R., "Mechanical and Chemical Contributions to the Erosion Rates of Graphite Throats in Rocket Motor Nozzles," *Journal of Spacecraft and Rockets*, Vol. 3, No. 10, 1966, pp. 1490–1494.
- ⁸Kays, W. M., and Crawford, M. E., "Convective Heat Transfer at High Velocities," *Convective Heat and Mass Transfer*, 2nd ed., McGraw-Hill, New York, 1980, pp. 300–310.